Journal of Power Sources 185 (2008) 1569–1574

Contents lists available at ScienceDirect

Journal of Power Sources

journal homepage: www.elsevier.com/locate/jpowsour

Nickel foam-based manganese dioxide–carbon nanotube composite electrodes for electrochemical supercapacitors

Jun Li[a], Quan Min Yang[b], Igor Zhitomirsky[a,*]

[a] Department of Materials Science and Engineering, McMaster University, 1280 Main Street West, Hamilton, Ontario, Canada L8S 4L7
[b] Inco Technical Services, Mississauga, Ontario, Canada L5K 1Z9

ARTICLE INFO

Article history:
Received 19 June 2008
Received in revised form 18 July 2008
Accepted 21 July 2008
Available online 30 July 2008

Keywords:
Manganese dioxide
Nanofibers
Carbon nanotubes
Nickel foam
Supercapacitor

ABSTRACT

Manganese dioxide nanofibers with length ranged from 0.1 to 1 μm and a diameter of about 2–4 nm were prepared by a chemical precipitation method. Composite electrodes for electrochemical supercapacitors were fabricated by impregnation of slurries of the manganese dioxide nanofibers and multiwalled carbon nanotubes (MWCNTs) into porous nickel foam current collectors. In the composite electrodes, MWCNT formed a secondary conductivity network within the nickel foam cells. Obtained composite electrodes, containing 0–20 wt.% MWCNT with total mass loading of 40 mg cm^{-2}, showed a capacitive behavior in the 0.1–0.5 M Na_2SO_4 solutions. The highest specific capacitance (SC) of 155 F g^{-1} was obtained at a scan rate of 2 mV s^{-1} in the 0.5 M Na_2SO_4 solutions. The SC increased with increasing MWCNT content in the composite materials and increasing Na_2SO_4 concentration in the solutions and decreased with increasing scan rate.

1. Introduction

Porous nickel foams are in high demand for applications in nickel–cadmium [1,2], nickel–metal hydride [1–4], nickel–zinc [5], lithium ion [6] batteries and electrochemical supercapacitors (ESs) [7]. In the batteries and supercapacitors, nickel foams are used as high surface area current collectors, containing highly accessible active material within their conducting light weight web, which provides structural strength.

Electrodes are produced by pasting a slurry of active material into a porous nickel foam, followed by impregnation, drying and calendering. The high porosity and large pore size of nickel foams allow for easy impregnation of the active material slurry into the porous current collectors. However, the increase in foam porosity resulted in reduced conductivity [1]. This problem has been addressed by the use of conductive additives, which formed a secondary conductivity network [1] within the nickel foam cells. The addition of nickel filaments [1] or carbon nanotubes [8] to the active material enabled enhanced conductivity for high power applications. The use of nickel foam current collectors for batteries allowed the fabrication of advanced electrodes [1–3] with lower internal resistance, better electrolyte access to active material and improved electrochemical performance.

The use of nickel foams for electrochemical storage devices has continued to expand to new applications, such as ES [9–12]. Manganese dioxides with various crystalline structures are promising active materials for ES [13–20]. Thin manganese dioxide films exhibited SC of ~700 F g^{-1} [21,22]. However, the SC decreased with increasing film thickness due to the low conductivity of MnO_2. Many successful efforts have been made in the area of the fabrication of composite materials and devices, where higher conductivity has been achieved by the use of carbon black, carbon nanotubes and other conductive additives [23–29]. The values of SC reported in the literature are usually in the range between 100 and 250 F g^{-1} for the material loadings of 0.4–0.5 mg cm^{-2} [30,31]. SC of 72 F g^{-1} in 0.1 M K_2SO_4 electrolyte was reported for composite manganese dioxide–acetylene black electrodes with material loading in the range of 10–40 mg cm^{-2} [27]. Manganese oxide–carbon nanotubes–acetylene black composites with material loading of 40 mg cm^{-2} showed a SC of 204.8 F g^{-1} in 1 M Li(Ac)–1 M $MgSO_4$ solutions [28]. The SC was calculated from a discharge curve at very low discharge rate using the mass of manganese dioxide and carbon nanotubes, without the mass of acetylene black and binder. However, obtained electrodes showed low cycling stability compared to excellent cycling stability reported in Ref. [27]. In another study [29] manganese oxide–carbon nanotubes–acetylene black composites with material loading of 10 mg cm^{-2} were prepared. In this approach manganese dioxide coatings were formed on carbon nanotubes by reduction of $KMnO_4$. The manganese oxide–carbon nanotubes–acetylene black composites showed a SC of 250 F g^{-1} in

* Corresponding author. Tel.: +1 905 525 9140; fax: +1 905 528 9295.
E-mail address: zhitom@mcmaster.ca (I. Zhitomirsky).

0378-7753/$ – see front matter © 2008 Elsevier B.V. All rights reserved.
doi:10.1016/j.jpowsour.2008.07.057

1 M KOH electrolyte. However, the control of the amount of MnO_2 in the composites prepared by this method presents difficulties. Moreover, the use of carbon nanotubes for the reduction of $KMnO_4$ usually results in the degradation of the carbon nanotubes due to the loss of carbon and formation of soluble carbonates [32]. The carbon loss and degradation of carbon nanotubes usually results in reduced conductivity. In this case conductive additives, such as acetylene black are necessary in order to improve the electrode performance [29]. The SC values for the composite materials [27–29] are far from the theoretical SC of $\sim 1370\,F\,g^{-1}$ [30] and reported experimental SC for thin films [21,22]. The capacitance of MnO_2 is believed to be predominantly due to pseudocapacitance as a result of redox processes associated with the surface adsorption of cations or incorporation of cations into the oxide structure [33,34]:

$$MnO_2 + C^+ + e^- \leftrightarrow MnO_2C \quad (1)$$

where $C^+ = Li^+$, Na^+, K^+, H^+. The development of ES requires the use of active materials with high surface area. Therefore, manganese dioxide nanofibers and carbon nanotubes with large surface area-to-volume ratio are of special interest for ES [35].

The goal of this work was the fabrication and investigation of composite electrodes containing manganese dioxide nanofibers and carbon nanotubes. In the approach described below, manganese dioxide nanofibers with high aspect ratio were prepared by a simple and low cost method. Composite electrodes containing two different types of fibrous materials were prepared using nickel foams as current collectors. We presented the results of electrochemical testing of the composite electrodes for applications in ES.

2. Experimental procedures

Manganese dioxide nanofibers were prepared by a chemical precipitation method described in a previous investigation [36]. The nanofibers showed poorly crystallized cryptomelane structure, and contained adsorbed water. The chemical composition was described by the formula $K_{0.14}MnO_{2+y}$, the mean oxidation state of Mn was found to be 3.7 [36]. MWCNT were provided by Arkema. Aqueous suspensions of manganese dioxide nanofibers and MWCNT were prepared using sodium dodecyl sulphate (Aldrich) as a dispersant. Prior to mixing together, the suspensions of manganese nanofibers and MWCNT were stirred and then ultrasonically agitated during 30 min. Mixed suspensions were stirred, washed with water and ultrasonically agitated during 30 min. INCOFOAM® substrates with a volumetric porosity of 95% were made by Inco using carbonyl technology [1]. The procedure for the slurry preparation and impregnation of the INCOFOAM® was similar to that described in a previous investigation [1]. The total mass of manganese dioxide and MWCNT in the composite electrodes was $40\,mg\,cm^{-2}$. The impregnated INCOFOAM® was roller pressed to ~20% of initial thickness in order to achieve final porosity of 30% [1].

Electron microscopy investigations were performed using a JEOL 2010F transmission electron microscope (TEM) and a JEOL JSM-7000F scanning electron microscope (SEM). Capacitive behavior of the composite electrodes was studied using a potentiostat (PARSTAT 2273, Princeton Applied Research) controlled by a computer using a PowerSuite electrochemical software. Electrochemical studies were performed using a standard three-electrode cell containing 0.1–0.5 M Na_2SO_4 aqueous solution, degassed with purified nitrogen gas. The counter electrode was a platinum gauze, and the reference electrode was a standard calomel electrode (SCE). Cyclic voltammetry (CV) studies were performed within a potential range of 0–1.0 V versus SCE at scan rates of $2–100\,mV\,s^{-1}$. The specific capacitance (SC) was calculated using half the integrated area of the CV curve to obtain the charge (Q), and subsequently dividing the charge by the total mass (m) of the composite material impregnated into nickel foam, and the width of the potential window (ΔV):

$$C = \frac{Q}{m\Delta V} \quad (2)$$

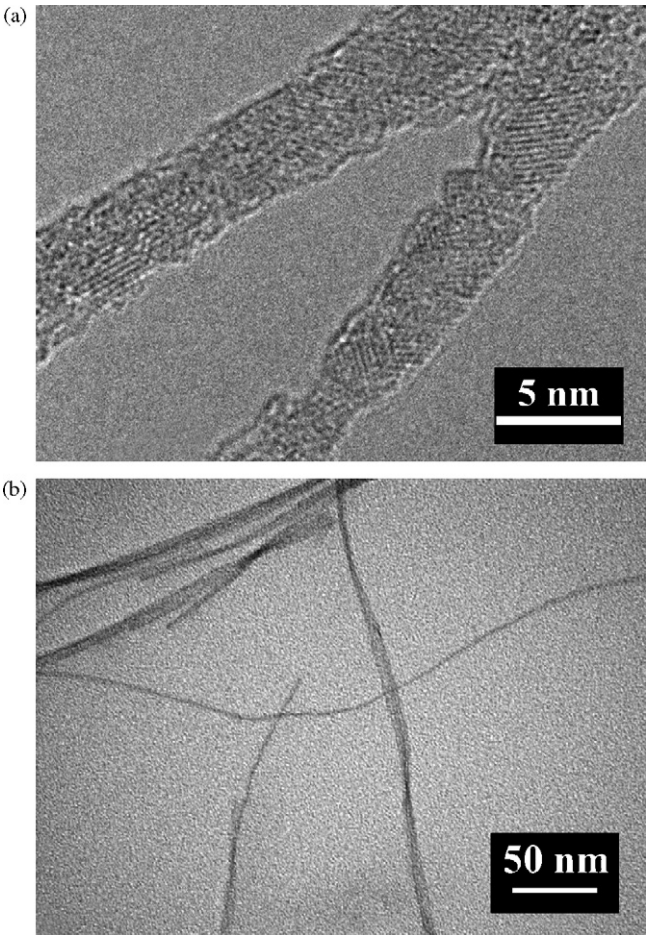

Fig. 1. (a and b). TEM images at different magnifications of the manganese dioxide nanofibers prepared by a chemical precipitation method.

3. Results and discussion

Fig. 1(a and b) shows TEM images of manganese dioxide nanofibers. The diameter of the manganese dioxide nanofibers prepared by the chemical precipitation method [36] was 2–4 nm and length 0.1–1 μm. Some nanofibers formed bundles, which contained several individual nanofibers (Fig. 1b). In the previous investigation [36], $0.05–0.16\,mg\,cm^{-2}$ films prepared by electrophoretic deposition on stainless steel foils, showed a capacitive behavior in a voltage window of 1 V. It was found that manganese dioxide nanofibers formed a porous fibrous network, which was beneficial for the electrolyte access to the active material. However, the SC decreased with increasing film thickness due to the low conductivity of the nanofibers.

The increase in conductivity can be achieved by the use of conductive additives. Moreover, high surface area current collectors, such as INCOFOAM®, enable better utilization of active materials [1]. It was suggested that composite materials containing manganese dioxide nanofibers and MWCNT had an advantage of improved contact between two different fibrous materials com-

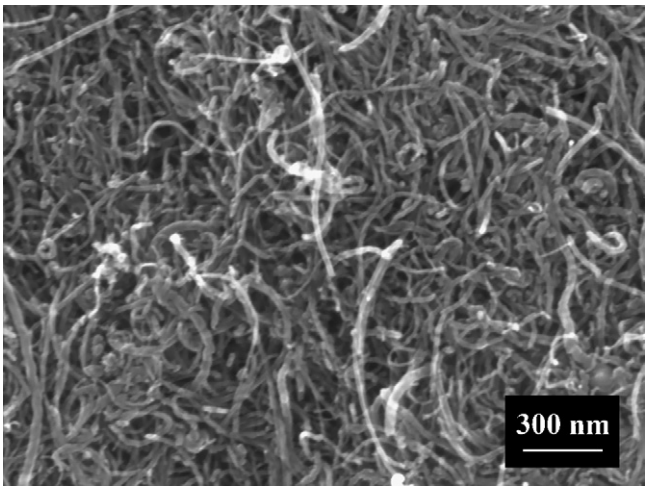

Fig. 2. SEM image of MWCNT.

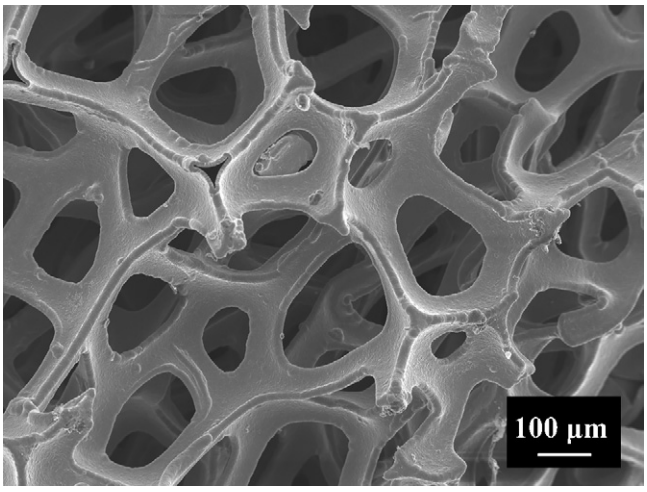

Fig. 3. SEM image of INCOFOAM®.

pared to composites of spherical particles of the same mass. The use of MWCNT as conductive additives has benefits of high surface area and low percolation threshold. According to the manufacturer, the average diameter of the MWCNT used in this study was ~15 nm and length ~0.5 μm (Fig. 2). The slurry containing two different fibrous materials was used for the impregnation of the INCOFOAM® (Fig. 3).

Fig. 4 shows SEM images of impregnated and roller pressed electrode. The SEM images at different magnifications of the electrode surface showed porosity (Fig. 4a and b). The SEM image of the fracture of the electrode (Fig. 4c) indicated that active material filled the voids in the nickel foam.

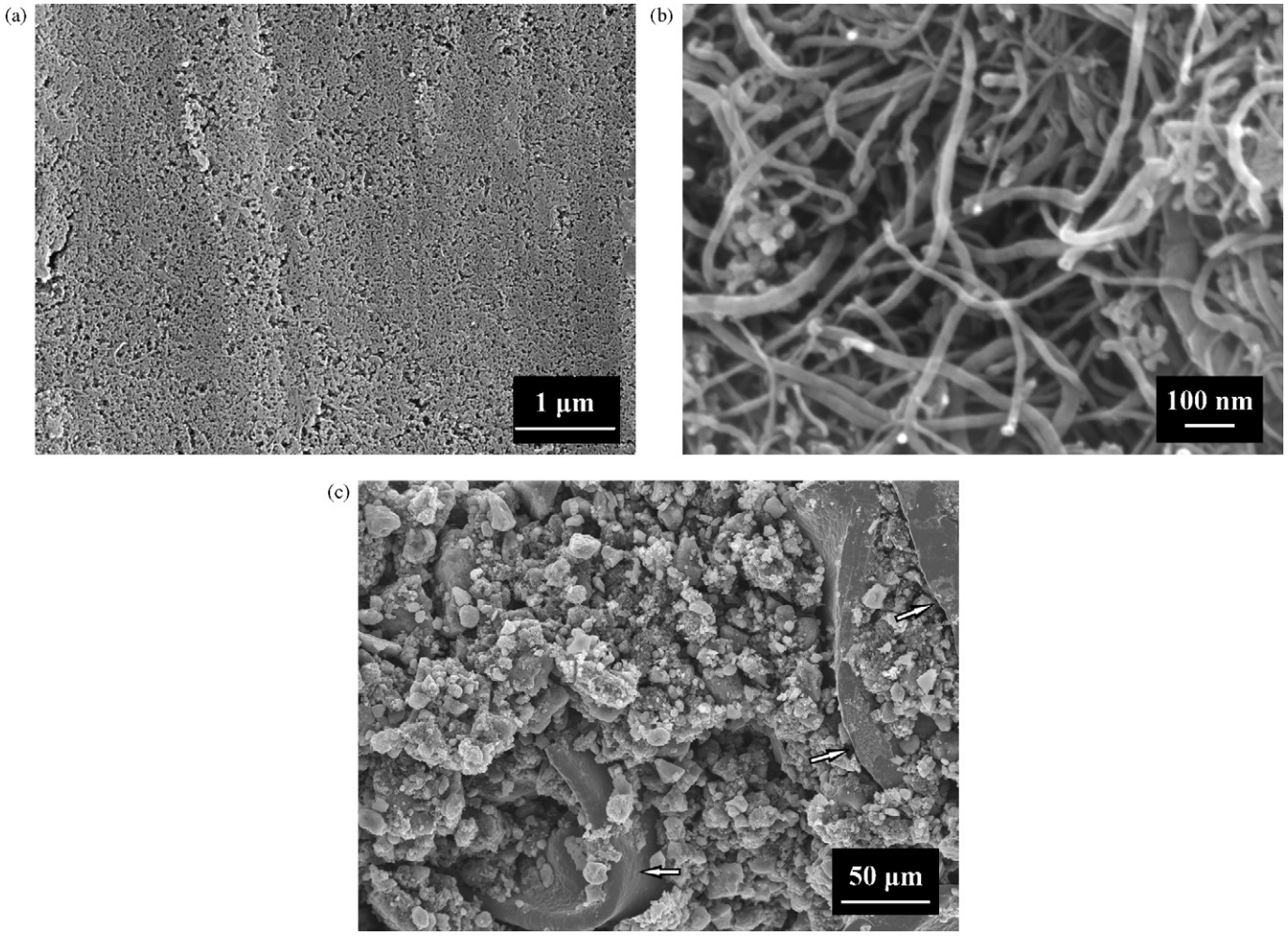

Fig. 4. (a, b and c). SEM images of a composite electrode, containing 15 wt.% of MWCNT. (a and b) Surface at different magnifications and (c) fracture. Arrows show Ni foam.

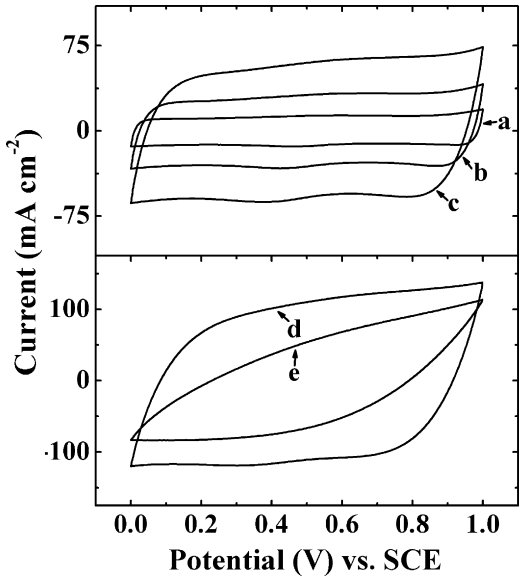

Fig. 5. CVs for the composite electrode, containing 15 wt.% MWCNT, tested at scan rates of (a) 2 mV s^{-1}, (b) 5 mV s^{-1}, (c) 10 mV s^{-1}, (d and e) 20 mV s^{-1} in (a–d) 0.5 M and (e) 0.1 M Na_2SO_4 solutions.

Electrochemical testing in the 0.1–0.5 M Na_2SO_4 solutions revealed capacitive behavior of the composite electrodes. Fig. 5 shows typical CVs at different scan rates. The box shape of the CVs and the increase in current with increasing scan rate indicated good capacitive behavior in the 0.5 M Na_2SO_4 solutions (Fig. 5a–d). However, the comparison of the CVs obtained at the scan rate of 20 mV s^{-1} in the 0.5 and 0.1 M Na_2SO_4 solutions (Fig. 5d and e) showed a smaller area of the CV obtained in the 0.1 M Na_2SO_4 solutions, which was related to lower SC. Moreover, the CV shape in the 0.1 M Na_2SO_4 solutions deviated significantly from the ideal box shape. The difference can be attributed to the lower conductivity of the 0.1 M Na_2SO_4 solutions and diffusion limitations in pores of the composite electrodes. This result is in a good agreement with the experimental data shown in Fig. 6. Higher SC was obtained in the 0.5 M Na_2SO_4 solutions compared to the 0.1 M Na_2SO_4 solutions for the samples of the same mass and composition. Therefore, further testing was performed in the 0.5 M Na_2SO_4 solutions. The highest SC of 155 F g^{-1} was obtained at a scan rate of 2 mV s^{-1} in the 0.5 M Na_2SO_4 solutions. The SC decreased with increasing scan rate for electrodes of fixed composition as shown in Fig. 6. The decrease

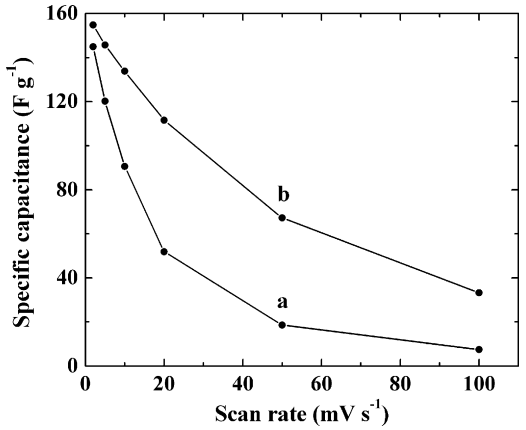

Fig. 6. SC vs. scan rate for composite electrodes containing 15 wt.% MWCNT tested in (a) 0.1 M and (b) 0.5 M Na_2SO_4 solutions.

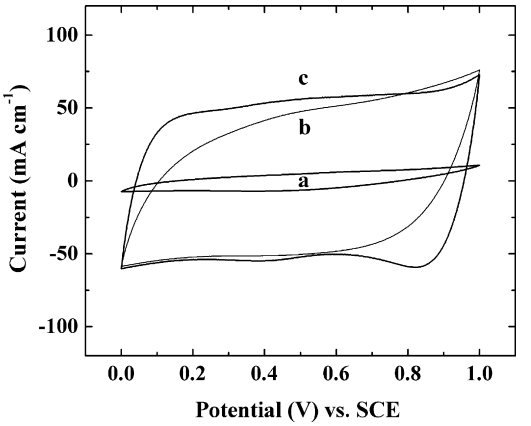

Fig. 7. CVs at a scan rate of 10 mV s^{-1} for composite electrodes containing (a) 0 wt.%, (b) 10 wt.% and (c) 20 wt.% MWCNT tested in the 0.5 M Na_2SO_4 solutions.

in SC with increasing scan rate can be attributed to the diffusion limitations in pores.

Fig. 7 shows the influence of active material composition on the capacitive behavior of the electrodes. For manganese dioxide electrodes, the relatively small area of the CV indicated poor capacitive behavior. The SC at a scan rate of 2 mV s^{-1} was only 22 F g^{-1} and decreased rapidly with increasing scan rate (Fig. 8). It should be noted that the same material deposited electrophoretically as a 0.05 mg cm^{-2} film [36] showed a box shape CV and a SC of 412 F g^{-1}. The difference can be attributed to different material loadings and insulating properties of the manganese dioxide. This result indicated that the conductivity of the Ni foam is insufficient at such materials loadings. The additional conducting network, provided by MWCNT, improved the capacitive behavior of the composite electrodes. The composite electrodes containing MWCNT showed box shape CVs (Fig. 7). The electrodes, containing 10 and 20 wt.% MWCNT, showed SC of 145 and 150 F g^{-1}, respectively, at a scan rate of 2 mV s^{-1}. It is important to note that the improvement in capacitive behavior with increasing MWCNT concentration was especially evident at higher scan rates (Fig. 8). The increase in MWCNT content from 10 to 20 wt.% resulted in increase in SC from 61 to 118 F g^{-1} at a scan rate of 20 mV s^{-1}, and from 32 to 79 F g^{-1} at a scan rate of 50 mV s^{-1}. The increase in SC can be attributed to increasing conductivity of the composite materials and changes in the composite microstructure associated with increasing MWCNT content from 10 to 20 wt.%. Recent studies showed that MWCNT can reduce the aggregation of nanoparticles of active material, inducing bet-

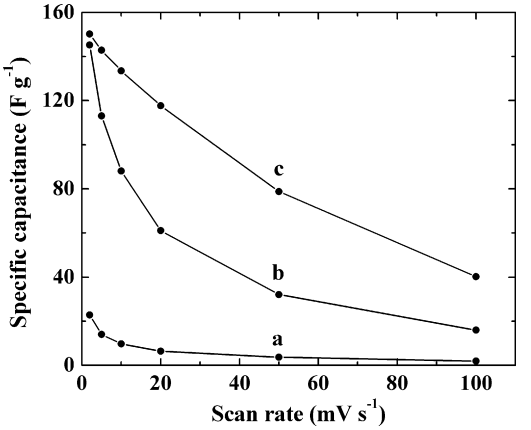

Fig. 8. SC vs. scan rate for composite electrodes containing (a) 0 wt.%, (b) 10 wt.% and (c) 20 wt.% MWCNT tested in the 0.5 M Na_2SO_4 solutions.

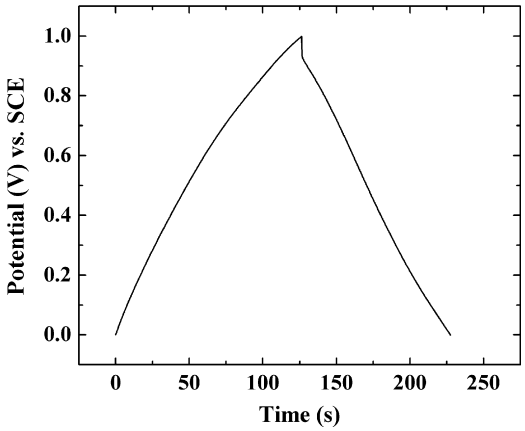

Fig. 9. Charge–discharge behavior at a current density 50 mA cm^{-2} for a composite electrode containing 20 wt.% MWCNT in the 0.5 M Na_2SO_4 solution.

ter distribution of the particles in the netlike MWCNT structure [37]. Reduced agglomeration of the particles resulted in improved electrochemical performance of the composite electrodes.

The increase in scan rate has a direct impact on the diffusion of ions, since at high scan rates ions approach only the outer surface of the electrode material [38]. The MWCNT content in the composite electrodes is an important factor controlling electronic conductivity of the materials. The investigation of NiO–MWCNT composites [39] showed the enhancement in the conductivity and SC for MWCNT content higher than the percolation limit of 10 wt.%. The investigation of manganese dioxide–MWCNT composites [40] showed that the 10–15 wt.% MWCNT additive increased the SC from 0.1 to 140 F g^{-1}. It was found that MWCNT generated an open mesoporous network which facilitated the electrolyte access to the active material. Moreover, extended polarization window was achieved in the manganese dioxide/MWCNT composites [40]. The study [40] highlighted the advantages of MWCNT compared to other conductive additives and showed improved capacitive behavior at a scan rate of 2 mV s^{-1}. Our testing results indicate that significant improvement in capacitive behavior can be achieved at higher scan rates when MWCNT are used as conductive additive for the fibrous manganese dioxide active material and using INCOFOAM® current collectors. The microstructure and composition of the composite electrodes can be further optimized by the variation of materials loading, electrode thickness, porosity and MWCNT content in the composites.

Fig. 9 shows charge–discharge behavior of the composite electrode at a current density of 50 mA cm^{-2}. The discharge curve is nearly linear, however initial voltage drop was observed, which can be attributed to electrode resistance. Fig. 10 shows complex impedance of the electrode in the frequency range of 100 mHz to 70 kHz. The equivalent circuit for electrochemical supercapacitors was discussed in detail by Conway [41]. The high frequency value of the real part of complex impedance has been used for the estimation of equivalent series resistance which was found to be ~0.5 Ω cm^2. It is suggested that the further optimization of electrode composition and microstructure will result in reduced resistance and improved capacitive behavior.

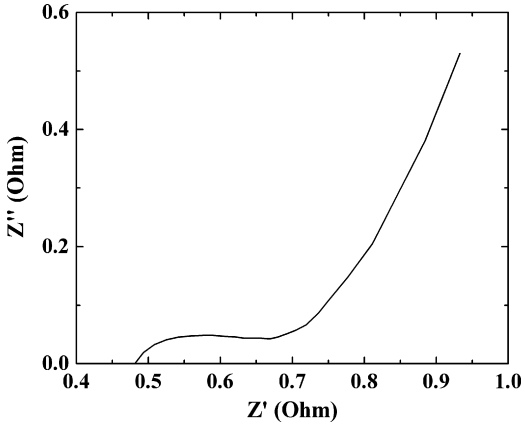

Fig. 10. Nyquist plot for complex impedance $Z^* = Z' - iZ''$ of the composite electrode containing 20 wt.% MWCNT in the 0.5 M Na_2SO_4 solution.

4. Conclusions

Composite electrodes for electrochemical supercapacitors, containing two different fibrous materials, were fabricated by impregnation of slurries of the manganese dioxide nanofibers and MWCNT into porous nickel foam current collectors. The composite electrodes with total mass loading of 40 mg cm^{-2} showed a capacitive behavior in the 0.1–0.5 M Na_2SO_4 solutions. Testing in the 0.5 M Na_2SO_4 solutions showed higher SC compared to the SC in the 0.1 M Na_2SO_4 solutions. MWCNT improved electrochemical performance of the electrodes by forming a secondary conductivity network within the nickel foam cells. The SC increased with increasing MWCNT content in the range of 0–20 wt.%, showing more distinct effect at higher scan rates, and decreased with increasing scan rate. The highest SC of 155 F g^{-1} was obtained at a scan rate of 2 mV s^{-1} in the 0.5 M Na_2SO_4 solutions.

Acknowledgements

The authors gratefully acknowledge the financial support of the Natural Sciences and Engineering Research Council of Canada and Vale Inco Limited.

References

[1] Q.M. Yang, V.A. Ettel, J. Babjak, D.K. Charles, M.A. Mosoiu, J. Electrochem. Soc. 150 (2003) A543–A550.
[2] V. Paserin, S. Marcuson, J. Shu, D.S. Wilkinson, Adv. Eng. Mater. 6 (2004) 454–459.
[3] D. Yan, W. Cui, J. Alloys Compd. 293–295 (1999) 780–783.
[4] M. Yao, K. Okuno, T. Iwaki, M. Kato, K. Harada, J.-J. Park, S. Tanase, T. Sakai, J. Electrochem. Soc. 154 (2007) A709–A714.
[5] T.-M. Waltraud, K. Karl, J. Power Sources 132 (2004) 275–281.
[6] Y. Yu, C.-H. Chen, J.-L. Shui, S. Xie, Angew. Chem. Int. Ed. 44 (2005) 7085–7089.
[7] A. Yuan, Q. Zhang, Electrochem. Commun. 8 (2006) 1173–1178.
[8] Q.S. Song, G.K. Aravindaraj, H. Sultana, S.L.I. Chan, Electrochim. Acta 53 (2007) 1890–1896.
[9] C. Yuan, X. Zhang, Q. Wu, B. Gao, Solid State Ionics 177 (2006) 1237–1242.
[10] M. Yao, K. Okuno, T. Iwaki, M. Kato, S. Tanase, K. Emura, T. Sakai, Electrochem. Solid-State Lett. 10 (2007) A245–A249.
[11] J.H. Park, S. Kim, O.O. Park, J.M. Ko, Appl. Phys. A 82 (2006) 593–597.
[12] I. Bispo-Fonseca, J. Aggar, C. Sarrazin, P. Simon, J.F. Fauvarque, J. Power Sources 79 (1999) 238–241.
[13] H.Y. Lee, J.B. Goodenough, J. Solid State Chem. 144 (1999) 220–223.
[14] J.-K. Chang, W.-T. Tsai, J. Electrochem. Soc. 150 (2003) A1333–A1338.
[15] C.-C. Hu, C.-C. Wang, J. Electrochem. Soc. 150 (2003) A1079–A1084.
[16] K.R. Prasad, N. Miura, J. Power Sources 135 (2004) 354–360.
[17] M.-S. Wu, P.-C.J. Chiang, Electrochem. Solid-State Lett. 7 (2004) A123–A126.
[18] N. Nagarajan, H. Humadi, I. Zhitomirsky, Electrochim. Acta 51 (2006) 3039–3045.
[19] K.-W. Nam, K.-B. Kim, J. Electrochem. Soc. 153 (2006) A81–A88.
[20] M. Nakayama, A. Tanaka, Y. Sato, T. Tonosaki, K. Ogura, Langmuir 21 (2005) 5907–5913.
[21] S.-C. Pang, M.A. Anderson, J. Mater. Res. 15 (2000) 2096–2106.
[22] S.-C. Pang, M.A. Anderson, T.W. Chapman, J. Electrochem. Soc. 147 (2000) 444–450.
[23] V. Khomenko, E. Raymundo-Piñero, F. Béguin, J. Power Sources 153 (2006) 183–190.
[24] V. Khomenko, E. Raymundo-Piñero, E. Frackowiak, F. Béguin, Appl. Phys. A 82 (2006) 567–573.
[25] T. Brousse, M. Toupin, R. Dugas, L. Athouël, O. Crosnier, D. Bélanger, J. Electrochem. Soc. 153 (2006) A2171–A2180.

[26] G.-X. Wang, B.-L. Zhang, Z.-L. Yu, M.-Z. Qu, Solid State Ionics 176 (2005) 1169–1174.
[27] T. Brousse, P.-L. Taberna, O. Crosnier, R. Dugas, P. Guillemet, Y. Scudeller, Y. Zhou, F. Favier, D. Bélanger, P. Simon, J. Power Sources 173 (2007) 633–641.
[28] Y. Wang, A. Yuan, X. Wang, J Solid State Electrochem. 12 (2008) 1101–1107.
[29] X. Xie, L. Gao, Carbon 45 (2007) 2365–2373.
[30] S. Devaraj, N. Munichandraiah, J. Electrochem. Soc. 154 (2007) A80–A88.
[31] J.-K. Chang, S.-H. Hsu, W.-T. Tsai, I.-W. Sun, J. Power Sources 177 (2008) 676–680.
[32] M.O. Danilov, A.V. Melezhyk, J. Power Sources 163 (2006) 376–381.
[33] C.-C. Hu, T.-W. Tsou, Electrochem. Commun. 4 (2002) 105–109.
[34] V. Subramanian, H. Zhu, B. Wei, J. Power Sources 159 (2006) 361–364.
[35] C. Kim, K.-S. Yang, W.-J. Lee, Electrochem. Solid-State Lett. 7 (2004) A397–A399.
[36] J. Li, I. Zhitomirsky, Mater. Chem. Phys., in press.
[37] Y.-G. Wang, L. Yu, Y.-Y. Xia, J. Electrochem. Soc. 153 (2006) A743–A748.
[38] R.K. Sharma, H.-S. Oh, Y.-G. Shul, H. Kim, J. Power Sources 173 (2007) 1024–1028.
[39] J.Y. Lee, K. Liang, K.H. An, Y.H. Lee, Synth. Met. 150 (2005) 153–157.
[40] E. Raymundo-Piñero, V. Khomenko, E. Frackowiak, F. Béguin, J. Electrochem. Soc. 152 (2005) A229–235.
[41] B.E. Conway, Electrochemical Supercapacitors, Kluwer Academic/Plenum Publishers, New York, 1999, pp. 479–556.